





Redox characterisation of Erv1, a key component for protein import and folding in yeast mitochondria

Efrain Ceh-Pavia¹, Xiaofan Tang^{1,2} , Yawen Liu³, Derren J. Heyes⁴, Bing Zhao³ , Ping Xiao²  and Hui Lu¹ 

1 Faculty of Biology, Medicine and Health, School of Biological Sciences, University of Manchester, UK

2 School of Materials, University of Manchester, UK

3 State Key Laboratory of Supramolecular Structure and Materials, Jilin University, Changchun, China

4 Manchester Institute of Biotechnology, University of Manchester, UK

Keywords

FAD-dependent enzyme; MIA pathway; reduction potential; sulfhydryl oxidase

Correspondence

H. Lu, Faculty of Biology, Medicine and Health, School of Biological Sciences, University of Manchester, Manchester M13 9PT, UK

Tel: +44 161 2751553

E-mail: hui.lu@manchester.ac.uk

(Received 29 June 2019, revised 8 October 2019, accepted 10 November 2019)

doi:10.1111/febs.15136

The mitochondrial import and assembly (MIA) pathway plays a vitally important role in import and oxidative folding of mitochondrial proteins. Erv1, a member of the FAD-dependent Erv1/ALR disulphide bond generating enzyme family, is a key player of the MIA pathway. Although considerable progress has been made, the molecular mechanism of electron transfer within Erv1 is still not fully understood. The reduction potentials of the three redox centres were previously determined to be -320 mV for the shuttle disulphide, -150 mV for the active-site disulphide and -215 mV for FAD cofactor. However, it is unknown why FAD of Erv1 has such a low potential compared with other sulfhydryl oxidases, and why the shuttle disulphide has a potential as low as many of the stable structural disulphides of the substrates of MIA pathway. In this study, the three reduction potentials of Erv1 were reassessed using the wild-type and inactive mutants of Erv1 under anaerobic conditions. Our results show that the standard potentials for the shuttle and active-site disulphides are approximately -250 mV and $-215 \sim -260$ mV, respectively, and the potential for FAD cofactor is -148 mV. Our results support a model that both disulphide bonds are redox-active, and electron flow in Erv1 is thermodynamically favourable. Furthermore, the redox behaviour of Erv1 was confirmed, for the first time using Mia40, the physiological electron donor of Erv1. Together with previous studies on proteins of MIA pathway, we conclude that electron flow in the MIA pathway is a thermodynamically favourable, smoothly downhill process for all steps.

Database

Erv1: [EC 1.8.3.2](#).

Introduction

All the mitochondrial intermembrane space (IMS) proteins are synthesised in the cytosol and most of them contain conserved Cys residues. Consequently, disulphide bond formation plays a key role during the

biogenesis of these IMS proteins [1,2]. They are synthesised in a Cys-unfolded and Cys-reduced form that is imported into mitochondrial IMS via a redox-sensitive pathway, called the mitochondrial import and

Abbreviations

ALR, augments liver regeneration; DTT, dithiothreitol; Erv, essential for respiration and viability; FAD, flavin adenine dinucleotide; IMS, intermembrane space; MIA, mitochondrial import and assembly; QSOX, quiescin sulfhydryl oxidase; TCEP, tris(2-carboxyethyl)phosphine.

assembly (MIA) pathway [3–6]. Erv1 (essential for respiration and viability 1) in yeast or called ALR (augmenter of liver regeneration in mammals [7–9]) is an essential component of the MIA pathway, and together with Mia40, catalyses oxidative folding of the newly imported IMS proteins [4,5]. Upon mitochondrial protein import, Mia40 acts as an oxidoreductase interacting with the substrate proteins directly and transfers a disulphide bond to the substrates via the formation of intermolecular disulphide linked complexes [10–13]. The reduced Mia40 is then re-oxidised by Erv1 (EC 1.8.3.2) for regeneration, and reduced Erv1 can be re-oxidised by molecular oxygen or oxidised cytochrome *c* [14].

Erv1 belongs to the Erv/ALR sulphhydryl oxidase family, having been identified in all mitochondria containing eukaryotes [8,15,16]. All these enzymes form a dimer and possess a highly conserved catalytic core domain of ~100 amino acids folded in a helix bundle and stabilised by noncovalently binding of flavin adenine dinucleotide (FAD) (Fig. 1) [17–19]. The catalytic (or FAD-binding) domain of yeast (*Saccharomyces cerevisiae*) Erv1 is at the C terminus. The FAD-binding domain also contains a redox active-site CXXC disulphide bond (Cys130–Cys133), which is also known as the proximal disulphide as it is located proximal to the isoalloxazine ring of FAD, and a CX₁₆C structural disulphide (Cys159–Cys176) [12,20,21]. Furthermore, Erv1 has a functionally important shuttle disulphide bond (Cys30–Cys33) in the nonconserved and unfolded N-terminal domain [12,22]. Studies have shown that the shuttle disulphide bond of Erv1 can be reduced by reduced Mia40 or disulphide reducing agents, for example dithiothreitol (DTT) and tris(2-carboxyethyl) phosphine (TCEP) [12,22]. The electrons are then transferred to the active-site (proximal) disulphide via formation of an intermediate disulphide (Fig. 1C, C33'–C130), the cofactor FAD, and then in turn the reduced Erv1 can be re-oxidised by transferring electrons to molecular oxygen (O₂) or cytochrome *c* for regeneration [14,23,24]. Thus, there are three redox-active centres in Erv1, the shuttle disulphide (C30–C33), active-site (proximal) disulphide (C130–C133) and the FAD cofactor. In addition, the Erv/ALR FAD-binding domain also exists in the endoplasmic reticulum of yeast (Erv2) [25], in poxviruses (E10R) [26] and in sulphhydryl oxidases of the extracellular environment (QSOX: quiescin sulphhydryl oxidase) [27].

The reduction potential ($E^{0'}$) of a redox compound is a key parameter for understanding electron transfer pathways in redox reactions. The higher oxidising power, the higher the reduction potential (less negative) is. A previous study by Dabir *et al.* [24] reported

the three reduction potentials of Erv1 to be –320 mV for the shuttle disulphide, –150 mV for the active-site disulphide and –215 mV for the FAD cofactor, respectively. However, the results raised some important questions. For example, why does the FAD of Erv1 have such a low (–215 mV) potential compared with other sulphhydryl oxidases [9,18,28]? These potential values would suggest that the electron flow from the active-site (proximal) disulphide to FAD was a thermodynamically unfavourable process in Erv1. Although very few studies have been reported, a similar phenomenon has not been observed for other well-characterised Erv/ALR enzymes, such as Erv2 and ALR [9,18]. However, the potential of Erv1 shuttle disulphide, located in the unfolded N-terminal domain, was shown to be –320 mV, suggesting it is a surprisingly stable disulphide bond and inconsistent with its function of acting as a redox active shuttle disulphide. It should be noted that the wild-type enzyme was used in the previous redox titration experiments [24]. This is likely to affect the measurements as the enzyme was active and would have altered the redox potential of the redox buffers, for example turned DTT to oxidised DTT (oxDTT) during sample incubation. Thus, it is important to re-evaluate the redox properties of Erv1 as it is a key and essential component for mitochondrial protein biogenesis.

To understand whether yeast Erv1 does have unique redox properties and to understand the thermodynamics of the electron flow in Erv1, in this study, we re-examined redox properties of yeast Erv1. The reduction potentials of the three redox centres in Erv1 were determined for the wild-type and an inactive double Cys mutant of Erv1. In addition, Erv1 redox titrations were carried out under anaerobic conditions using both chemical reductants and, for the first time, Mia40, the physiological electron donor of Erv1. Our results showed that the FAD cofactor has the most positive (less negative) reduction potential (–148 mV) of the three redox centres of Erv1, and the two disulphide bonds have a very similar value of reduction potential (about –215 ~ –260 mV). Together with previous studies, we conclude that electron flow in the MIA pathway is a smoothly downhill process over all the steps.

Results and Discussion

Electron titration of Erv1 under anaerobic conditions

In order to know how many electrons are required to fully reduce the FAD cofactor of Erv1, a dithionite

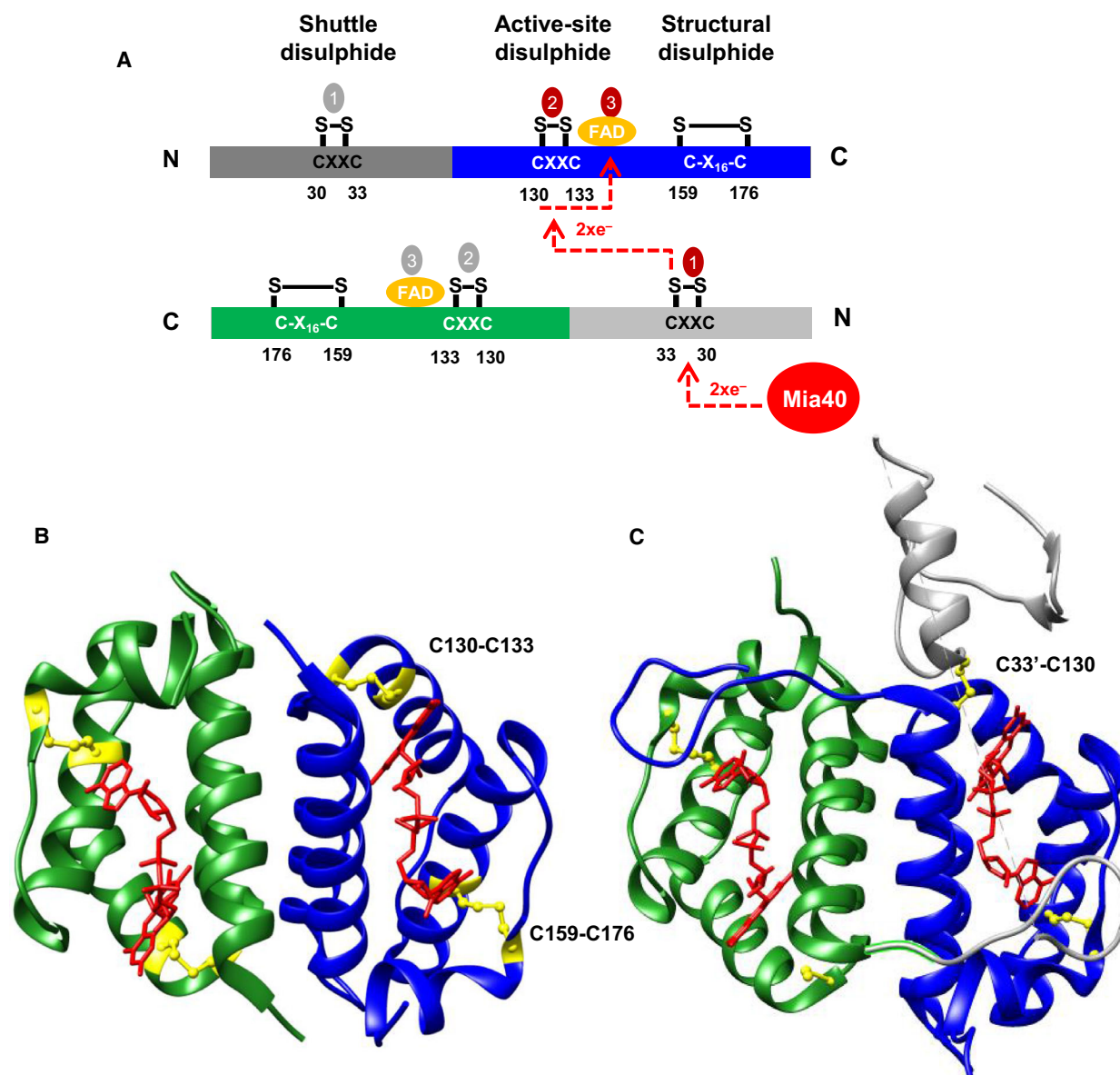


Fig. 1. Structure and redox centres of yeast Erv1. (A) Schematic structure of Erv1 with electron flow from Mia40 to Erv1 and between the three redox centres (red/grey cycles 1–3) of Erv1 dimer shown. (B) X-ray structure of the C-terminal domain of Erv1 (the PDB code is 4E0H) [19] with the active-site (proximal) disulphide and the structural disulphide shown in yellow, and FAD shown in red stick. (C) X-ray structure of Erv1C30,133S mutant (the PDB code is 4E0I) [19] with interdomain intermediate C33'-C130 disulphide and the structural disulphide shown in yellow, and FAD shown in red stick. The protein structures were produced using CHIMERA 1.14 program (San Francisco, CA, USA). PDB, Protein Data Bank.

titration under anaerobic conditions was performed and followed by UV-Vis spectra measurement (Fig. 2). Methyl viologen was added to mediate the transfer of reducing equivalents between dithionite and FAD of Erv1. The absorbance intensity of the FAD decreases at 460 nm upon reduction and was plotted against the number of electron equivalents (Fig. 2B). The decrease showed a linear dependence on the number of electrons with about 85% FAD reduction followed a

linear line with a slope of -0.49 . Thus, approximately 2 electrons were transferred per FAD initially. Subsequently, the FAD reduction became less efficient and (at least) another two electrons were required for the remaining $\sim 15\%$ FAD. Hence, four-electron equivalents of dithionite are required to fully reduce the two-electron acceptor FAD. On the other hand, only two electrons were required to reduce the Erv1C130,133S double Cys mutant as shown in Fig. 2C. These results

suggest that not only the FAD of Erv1 was reduced, but the proximal redox-active disulphide bond was reduced as well during the later stage of the titration of the WT Erv1. Our results also showed that the reduction potential of Erv1 proximal disulphide could be determined using dithionite titration. It should be noted that the appearance of the absorption peak at about 550–650 nm indicates the presence of the blue neutral semiquinone of FAD, similar to that of ALR [9].

Reduction potential of the cofactor FAD

After it was established that both the FAD and the proximal disulphide (C130-C133) of Erv1 could be reduced by dithionite titration, we repeated the titration experiment with more data points and in the presence of a range of redox mediators (see [Materials and methods](#)) to simultaneously measure both the electron potential and UV-visible absorbance spectra (Fig. 3A). The relative absorbance intensity at 460 nm was plotted against electron potential, and the data were analysed using the Nernst equation (Fig. 3B). The analysis gave an apparent midpoint potential E_m of -150 ± 5 mV for a 2-electron reduction of Erv1 (black line). Clearly, not all the data points can be fitted to the equation single 2-electron reaction, it may

partially due to the accumulation of semiquinone intermediate (Fig. 3B, insert). In particular, when redox potential was more reducing (negative) than -160 mV, the data points were clearly away from the fitted line. This result was consistent with the above conclusion that the proximal disulphide was reduced in parallel with the FAD at the later stage of FAD reduction (Fig. 2B). Furthermore, we analysed the data with Nernst equation for a two 2-electron (2x2e) reaction, which fitted the data very well (red line) with two standard reduction potentials of -148 ± 5 mV (FAD) and $-215 \text{ mV} \pm 5 \text{ mV}$ (disulphide bond) were determined. Moreover, the same experiment was performed with Erv1C30,33S (Fig. 3C) and Erv1C130,133S (Fig. 3D) double Cys mutants. Whilst two reduction potentials of -145 mV (for FAD) and -271 mV (disulphide bond) were determined for Erv1C30,33S, one reduction potential of -212 mV (for FAD) was determined for Erv1C130,133S. The results confirmed that (a) it was the shuttle disulphide bond that was reduced during the later stage of FAD reduction, and (b) mutation of the proximal disulphide (C130-C133), but not the shuttle disulphide, affected the reduction potential of FAD cofactor. Thus, we signed the potentials of -148 ± 5 mV for FAD of Erv1. This reduction potential is similar to that reported for human sfALR (-178 mV), QSOX

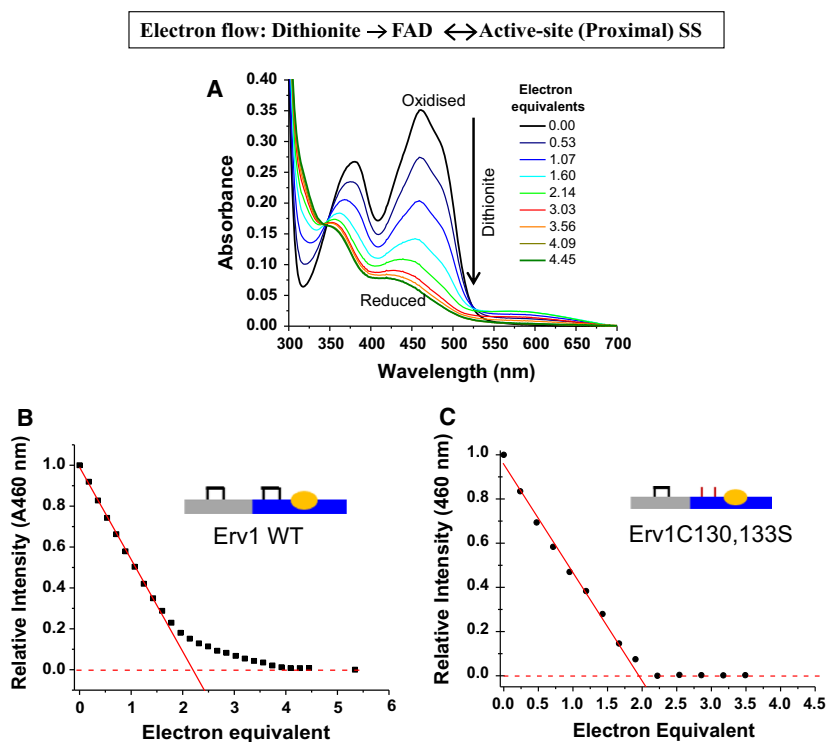


Fig. 2. Electron titration of FAD in Erv1. (A) UV-visible absorbance spectra of Erv1 recorded before (black line) and after addition of sodium dithionite at various electron equivalents (electrons/FAD) under anaerobic conditions. Absorbance spectra of FAD at fully oxidised (black) and fully reduced (olive green) were shown in thick lines. (B) Normalised absorbance at 460 nm vs. electron equivalents for the data shown in A. The red line represents a linear fit to the early data points with a slope of -0.49 . About four electrons were required to fully reduce FAD. The value represents the average of two independent experiments. (C) As in (B) but normalised sodium dithionite titration curve for Erv1C130,133S mutant. The red line represents a linear fit to the early data points with a slope of -0.49 . About two electrons were required to reduce FAD.

(-153 mV), and it is a bit more positive than that reported for Erv2 (-200 mV), an ER localised sulphhydryl oxidase in yeast [9,18,28].

Reduction potential of the proximal disulphide

A proximal disulphide in direct redox communication with the FAD isoalloxazine is a key feature shared by all the disulphide oxidoreductases. The reduction potential of this disulphide is hard to measure due to its active communication with the FAD cofactor. Based on our results above (Fig. 3), the reduction potential of C130-C133 was estimated to be between -200 and -300 mV. To verify this, we repeated the titration with Erv1C30,33S, and the redox state of the proximal disulphide bond (C130-C133) was analysed using AMS thiol-modification assay. As shown in

Fig. 4, a small fraction of Erv1 was reduced start from reduction potential of about -180 mV and more was reduced with the addition of dithionite hence at more negative potential. An apparent reduction potential of -260 ± 5 mV was determined for the proximal disulphide bond (C130-C133), similar to that determined from Fig. 3C. Thus, the results of our two independent methods showed that the reduction potential of the proximal disulphide is at about -215 mV (in the WT, C30-C33 disulphide bonded) to -260 mV (in C30,33S mutant) with an average of -238 mV. It is ~ 90 mV more reducing (negative) than the FAD of Erv1 (-148 mV). There is a clear difference between the results obtained by using the WT (-215 mV) and Erv1C30,33S mutant (-260 mV), which may be caused by changes in protein conformation and/or interactions between the N-terminal and C-terminal

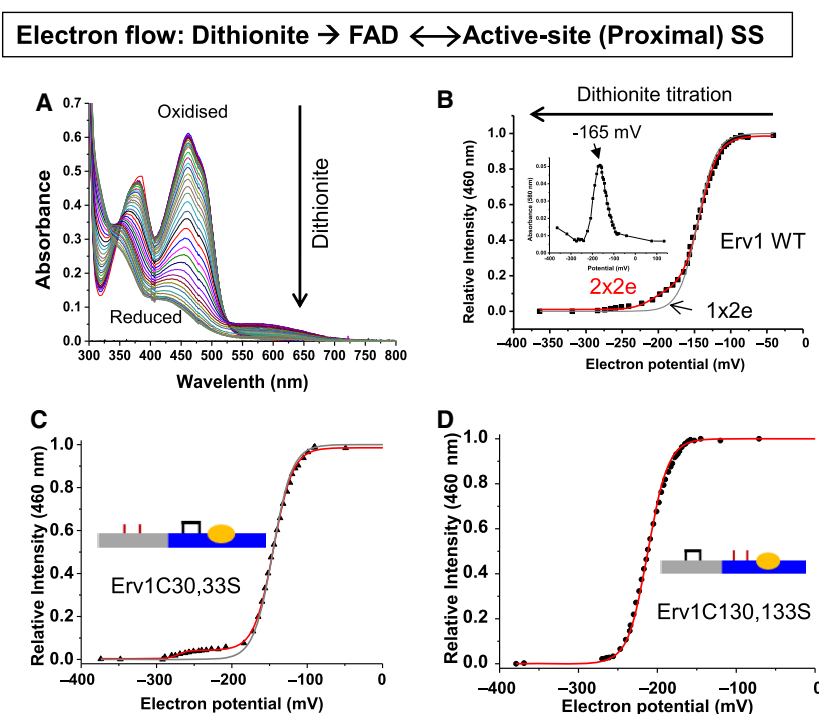


Fig. 3. FAD redox potential titration of Erv1. (A) Representative UV-visible absorbance spectra of Erv1 recorded at various electron potentials during dithionite titration under an anaerobic condition. FAD goes from fully oxidised (top, black line) to fully reduced (bottom, olive green line). (B) Normalised absorbance at 460 nm vs. electron potential for the WT Erv1 data shown in A. The data were fitted using Nernst equation for one 2-electron (1x2e, black line) and two 2-electron (2x2e, red line) reactions, respectively. A standard reduction potential of -150 ± 5 mV for 1x2e was obtained, whilst two standard reduction potentials of -148 ± 5 and -215 ± 5 mV for 2x2e were determined. The values represent average of two independent experiments. The insert is a plot of intensity at 580 nm vs. electron equivalents for the data shown in A. (C) As described in B but for Erv1C30,33S mutant. The data were best fitted with a Nernst equation for 2x2e reaction with two reduction potentials of -145 and -271 mV obtained (red line). (D) As in described in B but for Erv1C130,133S mutant. The data were best fitted to a Nernst equation for a 1x2e reaction with a reduction potential of -212 mV obtained (red line).

domains due to C30,33S mutation. Without the shuttle disulphide bond, the flexible N-terminal domain could exist in a different conformation and be primed for interaction with the proximal disulphide, which may result in the potential of the proximal disulphide shifted shifting from -215 to -260 mV. Thus, our results showed that the proximal disulphide bond (C130-C133) has a reduction potential about -215 (-215 mV \sim -260 mV), and interestingly depends on the redox state or conformation of the shuttle disulphide bond. This is consistent with our result that four (not six) electrons are required to reduce Erv1 FAD fully (Fig. 2B).

It is experimentally challenging to determining the potential of an active-site (proximal) disulphide of Erv1/ALR or Erv domain-containing enzyme due to its activity. It was determined to be -235 mV for the human sfALR [29] and -273 mV for QSOX [28] by using the more reducing FAD homologue 5-deaza-FAD substituted enzymes. These values are similar to our result of Erv1 proximal disulphide (-215 \sim -260 mV) determined in this study.

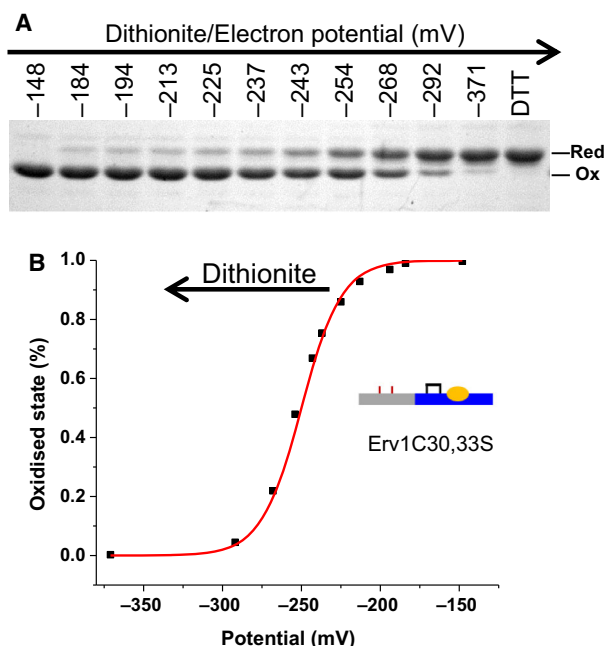


Fig. 4. Redox state analysis of the proximal disulphide bond of Erv1 with Erv1C30,33S mutant. (A) SDS/PAGE of an AMS assay of Erv1C30,33S taken at various potentials along a FAD dithionite titration under an anaerobic condition. Positive control: the protein was treated with 1 mM DTT and then 10 mM AMS. (B) Quantification of data shown in A and analysed using Nernst equation with a reduction potential of -260 ± 5 mV was obtained from two independent experiments.

In summary, in contrast to the previous report by Dabir *et al.* [24] that the proximal disulphide (C130-C133) of Erv1 was less reducing than FAD, our results show that C130-C133 is more reducing and thus electron flow from the proximal disulphide to the FAD is a thermodynamically favourable downhill reaction. Our conclusion is consistent with that of human ALR and QSOX that were both reported to perform a thermodynamically favourable downhill reaction during electron flow from the proximal disulphide to the FAD cofactor.

Reduction potential of the shuttle disulphide

A solvent-accessible redox-active disulphide bond often has a reduction potential around -200 mV. Such as the E^0 of glutathione (GSH/GSSG) is -240 mV at pH 7.0, about -120 mV for the most oxidising DsbA CXXC disulphide, and about -270 mV for the most reducing Trx CXXC disulphide [30–32]. On the other hand, many substrate proteins of the MIA pathway have reduction potentials around -310 to -340 mV for their stable structural disulphides [33–37], and it is about -290 mV for yeast Mia40 CPC [37]. The previously measured reduction potential of the Erv1 shuttle disulphide was -320 mV [24], which seems to be too stable and inconsistent with its function as shuttle disulphide bond [12]. In this study, we re-measured the reduction potential of the Erv1 shuttle disulphide with the inactive Erv1C130,133S double Cys mutant coupled with the AMS assay (Fig. 5). Redox buffer at various potentials was prepared using GSH/GSSG or DTT/oxDTT as described previously [24]. After incubation for 3 h, the samples were TCA precipitated before AMS assay and analysed using nonreducing SDS/PAGE (Fig. 5). A reduction potential of -250 mV was obtained for the shuttle disulphide of Erv1, which is slightly more negative but similar to that of the active-site (proximal) disulphide (-215 \sim -260 mV). Our result of the shuttle disulphide is clearly different from -320 mV published by Dabir *et al.* [24]. We reasoned this difference may be due to different proteins (WT vs. C130,133S mutant) or data analysis. To address this, we reanalysed our data using $[GSH]/[GSSG]$ rather than $[GSH]^2/[GSSG]$ in the Nernst equation and a reduction potential of -318 mV was obtained, which may explain the difference. We also tried to repeat the measurement with WT Erv1, but did not get a clear result, possibly (partially) due to recycling of the active enzyme. On the other hand, the difference may also reflect a redox change due to conformation change caused by the C130,133S mutation. This is less likely as the proximal

Cys residues are located in a folded domain and the shuttle Cys are in an unfolded domain, and a reduction potential of -320 mV is too stable for disulphide bond in unfolded protein domain.

Verification of Erv1 redox parameters using reduced Mia40 as electron donor

Dithionite is a convenient and commonly used chemical electron donor for FAD reduction studies. In practice, Mia40 is the physiological electron donor or upstream substrate of Erv1/ALR enzymes in mitochondria, and it reduces Erv1 via the shuttle and active-site (proximal) disulphide bonds to FAD (Fig. 6). Since our result is different from the previous result by Dabir *et al.* [24] in terms of the relative reduction potentials between the proximal disulphide and FAD cofactor, we carried out Erv1 reduction titration using reduced Mia40. The functional C-terminal domain of Mia40 was reduced (rMia40c) by incubation of the purified protein with 0.5 mM TECP as described previously [21], and followed by buffer exchange inside an anaerobic glove box to remove TCEP and molecular oxygen. The UV-visible spectra of Erv1 were measured during rMia40c titration and are shown in Fig. 6. The absorbance of the FAD decreased with the increase of rMia40c linearly with a slope of about 1.0 until about 60% FAD was reduced, showing that the two electrons from rMia40c flowed

to the FAD at a molar ratio of 1 : 1 initially. The remaining FAD reduction was slowed down consistent with above observation of reduction of the FAD and disulphide bonds in parallel. These results confirmed that the FAD cofactor has the most positive (less negative) reduction potential amongst the three redox centres of Erv1. Furthermore, no peak around 580 nm was observed during rMia40c titration, and thus, no semiquinone accumulation was detected when the physiological substrate Mia40 was used to reduce Erv1. This result suggests that the blue neutral semiquinone accumulation observed during dithionite titration of Erv1 and many other FAD-dependent enzymes may be an artefact of chemical reduction, which may need to be re-evaluated in some cases.

Conclusion

The overall aim of this study was to investigate the thermodynamic mechanism regulating the electron flow in the mitochondrial sulphhydryl oxidase Erv1. The reduction potentials of three redox centres in Erv1 were determined to be: -250 ± 5 mV for the shuttle disulphide bond (C30-C33), -215 to -260 mV for the proximal disulphide bond (C130-C133) and -148 ± 5 mV for the FAD cofactor (Fig. 7). Interestingly, the redox potential of the proximal disulphide seems to depend on the redox state of the shuttle disulphide bond. Furthermore, the physiological substrate Mia40 was used to confirm that

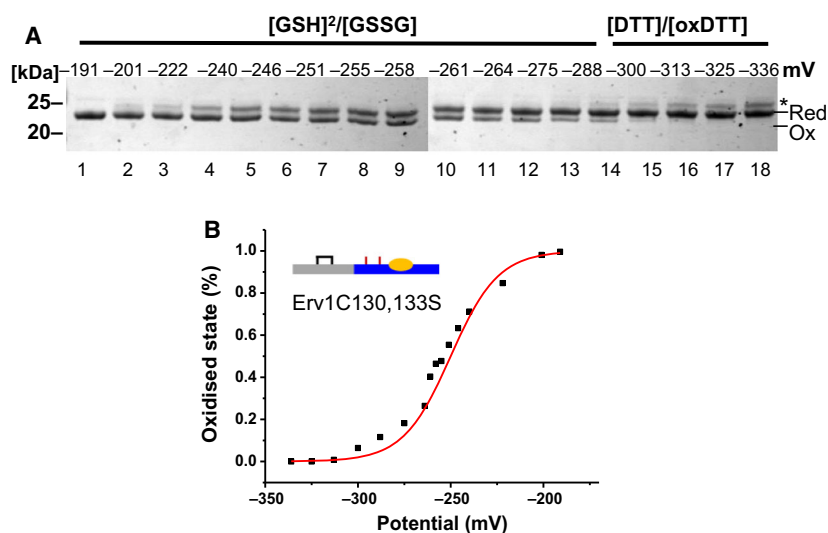


Fig. 5. Redox state analysis of the shuttle disulphide bond of Erv1 with Erv1C130,133S mutant. (A) SDS/PAGE of an AMS assay of Erv1C130,133S taken after incubation in a redox buffer at various redox potentials (lanes 2–17). Lane 1: Oxidised control of untreated protein; lane 18: Reduced control of the protein pretreated with 1 mM DTT and then 10 mM AMS. The * indicates a band with the structural disulphide bond reduced as well. (B) Quantification of data shown in A and analysed using Nernst equation with a reduction potential of -250 ± 5 mV was obtained based on two independent experiments. Each corresponding potential was calculated based on using $[GSH]^2/[GSSG]$ or $[DTT]/[oxDTT]$ in the Nernst equation.

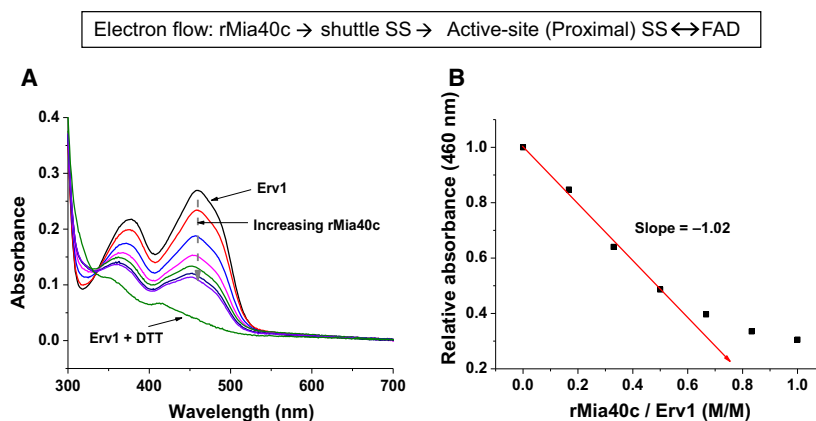


Fig. 6. Reduction of Erv1 by rMia40c titration under anaerobic condition. (A) UV-Vis Spectra of Erv1 in the absence (top, black line) and presence of various amount of rMia40c, together with the FAD fully reduced spectra (Erv1 + DTT, olive green). (B) Plot of normalised absorbance at 460 nm vs the molar ratio of rMia40c/Erv1 for the data shown in A. The normalisation was based on the intensity of fully oxidised Erv1 (in the absence of rMia40c) as 1 and the DTT reduced Erv1 as 0. The red line represents a linear fit with the early data points of the titration, with a slope of 1.0 obtained.

the FAD has the most positive (less negative) reduction potential in Erv1, and no semiquinone accumulation was observed during the Mia40-Erv1 reduction. Together with previous studies, we conclude that electron flow in the MIA pathway is a thermodynamically favourable smoothly downhill process over all the steps, from the upstream imported substrate proteins to Mia40-Erv1 and to the downstream electron acceptors (Fig. 7).

Materials and methods

Materials

All chemicals used in this study were analytical grade and were from Sigma-Aldrich Inc. (St. Louis, MO, USA) or Thermo Fisher Scientific (Waltham, MA, USA) unless specified. All solutions prepared using MilliQ water. Unless specifically stated, all experiments in this study were carried out in a buffer called BAE (50 mM Tris/HCl, 150 mM NaCl, 1 mM EDTA, pH 7.4) at 25 °C.

Protein purification

For Erv1 (the WT and mutants), the pET-24a(+) plasmid containing yeast ERV1 gene was expressed in *Escherichia coli* Rosetta-gamiTM 2 cells (Novagen, Merck KGaA, Darmstadt, Germany) and purified using Ni-NTA (Ni²⁺-nitrilotriacetate) His-bind beads (Novagen) as described previously [12,21,38]. Further purification was done by size-exclusion chromatography (SEC) using buffer AE (BAE: 50 mM Tris/HCl, 150 mM NaCl and 1 mM EDTA, pH 7.4) on a Superdex 200 or Superdex 200plus 100/300 GL column (GE Healthcare Bio-sciences, Uppsala, Sweden). Similarly, Mia40c (C-domain of Mia40: residues 284–403) was

expressed in *Escherichia coli* Rosetta-gamiTM 2 cells (Novagen) and purified using Ni-NTA beads [21,39]. Superdex 75 100/300 GL column was used to further purify and isolate the monomer proteins for this study.

Preparation of reduced Mia40c (rMia40c)

Purified Mia40c was incubated with 0.5 mM Tris(2-carboxyethyl)phosphine (TCEP) for at least 10 min at 25 °C as described previously [21]. Excess TCEP was removed using a PD-10 column pre-equilibrated with anaerobic buffer BAE (BAE: 50 mM Tris/HCl, 150 mM NaCl, 1 mM EDTA, pH 7.4) inside an anaerobic glove box (Belle Technology, Weymouth, UK), with oxygen levels maintained below 2 p.p.m. Buffers were made anaerobic by extensive bubbling with oxygen-free nitrogen, prior to incubation inside the anaerobic glove box. The concentration of rMia40c was determined using a ϵ_{280} of 11.7074 $\text{mm}^{-1}\cdot\text{cm}^{-1}$ as predicted using the PROTPARAM software.

Erv1 reduction under anaerobic conditions

For all anaerobic experiments, the assays were done within an anaerobic glove box (Belle Technology), with oxygen levels maintained below 2 p.p.m. Buffers were made anaerobic by extensive bubbling with oxygen-free nitrogen, followed by incubation inside the anaerobic glove box. Proteins were buffer exchanged using PD-10 column to anaerobic BAE in an anaerobic glove box, before each experiment.

FAD electron titration with dithionite

Electron titrations of the FAD cofactor in Erv1 were conducted in BAE using protein concentrations (based on bound FAD) ranging from 30 to 60 μM . A freshly

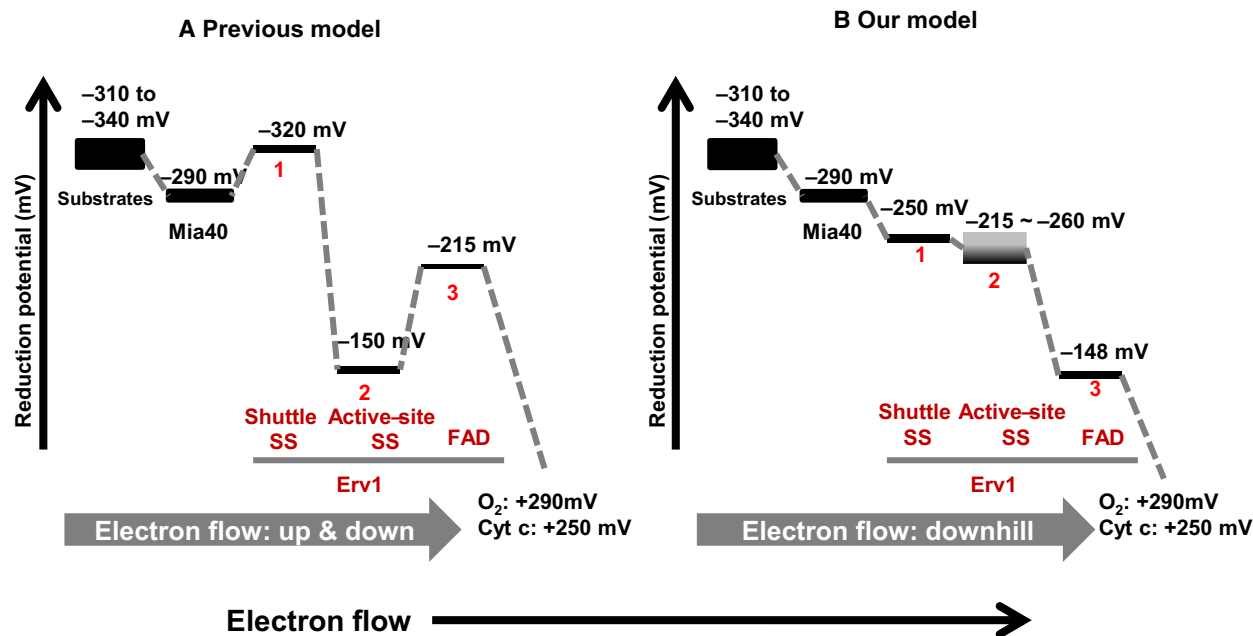


Fig. 7. Schematic energetic landscape of the MIA pathway. The reduction potentials for known substrates, Mia40 and three redox centres of Erv1 are shown. In the previous model (A), electron flows up and down between Mia40 and Erv1 and within Erv1. In our model (B), electron flows smoothly downhill over all the steps of the MIA pathway.

made sodium dithionite solution was titrated using an anaerobic FAD solution of known concentration ($\epsilon_{450} = 11.3 \text{ mM}^{-1}\cdot\text{cm}^{-1}$). This titration was done before and after the Erv1 assays to obtain an average normality. Small known volumes (0.5–2 μL) of dithionite solution were then used to reduce the protein. The UV-visible spectrum was recorded from 250 to 700 nm after each addition (equilibration time of 10–15 min) using a Cary 50 Bio UV-visible spectrophotometer. The point at which the reduction of FAD was complete (no further decrease in absorbance at either 460 nm) marked the number of electrons required for complete FAD reduction. The relative absorbance change at 460 nm was normalised with the value of the fully oxidised FAD set as 1 and the value of the fully reduced FAD as 0. The results are the average of two independent experiments.

FAD reduction potential titration with dithionite

Electron potential measurements were conducted in BAE with protein concentrations (based on bound FAD) of 30–80 μM . Mediators for improved conductivity between the protein and electrode were added. Typically, these were (final concentrations) 2 μM phenazine methyl sulphate [$E_{1/2}$ 80 mV vs normal hydrogen electrode (NHE)], 7 μM 2-hydroxy-1,4-naphthoquinone ($E_{1/2}$ –145 mV vs NHE), 1 μM benzyl viologen ($E_{1/2}$ –311 mV vs NHE) and 0.3 μM methyl viologen ($E_{1/2}$ –430 mV vs NHE). Sodium dithionite solutions (in BAE) were made up fresh inside the glove box immediately before the experiment. Small volumes

(0.5–5 μL) of the solution were gradually added to reduce the protein (5 mL). Adequate time (10–20 min) was allowed for electronic equilibration following each addition of reductant, and prior to the spectrum being recorded at a stabilised reduction potential. Spectra were recorded from 300 to 800 nm using a fibre optic probe (Varian) immersed in the protein solution and connected to a Cary 50 Bio UV-visible spectrophotometer. The electron potential was monitored using a Seven Easy pH meter (METTLER TOLEDO, Leicester, UK) with a Pt/Calomel electrode and a correction factor of +240 mV to adjust the electron potential. The protein was mixed slowly throughout the assay using an 8.5 mm magnetic flea on a magnetic stirrer.

The relative absorbance change at 460 nm was normalised with the value of the fully oxidised FAD set as 1 and the value of the fully reduced FAD as 0. To calculate the standard redox potentials, the collected data were fitted to the Nernst equation with the number of electrons restricted to $z = 2$. For two 2-electron reaction analysis, the following equation was used:

$$Y = \frac{A1 \times 10^{X-E1 \times (2/59)} + A2 + A3 \times 10^{E2-X \times (2/59)}}{1 + 10^{X-E1 \times (2/59)} + 10^{E2-X \times (2/59)}}$$

where A1–A3 are amplitudes of relative absorbance change, E1 and E2 are the standard reduction potentials. The results represent the average of three independent experiments. The fittings were done using the Origin 8.5 software.

AMS thiol modification assay

Thiol-disulphide redox state was analysed using the agent 4-acetamido-4'-maleimidylstilbene-2,2'-disulphonic acid (AMS). The thiol-modifier AMS (Molecular Probes, Thermo Fisher Scientific) covalently reacts with any free thiols resulting in an increase in the molecular weight of 0.5 kDa per thiol. For the proximal disulphide potential determination, Erv1C30,33S mutant was used. The protein samples were taken along the dithionite redox titration experiment and mixed with an equal volume of anaerobic 2X non-reducing SDS/PAGE sample buffer containing 2 mM AMS. The positive control for complete reduction of the Erv1 disulphide was made by incubating the protein with 1 mM DTT under anaerobic condition for 10 min followed by incubation with 2 mM AMS and nonreducing sample buffer, in dart for about 10 min. For the shuttle disulphide potential determination, Erv1C130,133S was used. A set of redox buffers from -180 to -360 mV was prepared using various ratios of reduced/oxidised glutathione (GSH/GSSG) or DTT/oxDTT as described previously [24]. The potentials of the redox buffers were calculated using Nernst equation and $[GSH]^2/[GSSG]$ or $[DTT]/[oxDTT]$, respectively. The $E_h^{0'}$ of -264 mV for GSH/GSSG and -354 mV for DTT/oxDTT at pH 7.4 was used. The proteins were incubated for about 3 h in the redox buffers saturated with nitrogen gas. After incubation for about 3 h, the reaction was quenched and the proteins were precipitated by the addition of TCA (10%) on ice for 30 min. The protein pellets were washed with acetone. Then, the precipitated proteins were solubilised and incubated in a buffer containing 2 mM AMS and nonreducing SDS/PAGE sample buffer, in dart for about 10 min. All samples were analysed using 16% tris-tricine SDS/PAGE, coomassie staining and band intensity qualification using IMAGEJ program.

Acknowledgments

We thank the funding supported by the Biotechnology and Biological Sciences Research Council (grant number BB/H017208), the Royal Society (IE150835), the Mexican National Council for Science and Technology (CONA-CyT) studentship for ECP and Chinese Scholarship Council (CSC) studentship for XT. Thanks Nigel Scruton and Andy Munro of the University of Manchester for their support and helpful comments during the project.

Conflicts of interest

The authors declare no conflict of interest.

Author contributions

All authors have contributed to experimental design and data analysis. ECP performed the experiments for

Figs 2–4; XT help with data analyse for Fig. 3 and did the experiments for Fig. 6; YL did the experiments for Fig. 5. DJH helped ECP and XT technically with the experiments under anaerobic conditions. HL wrote the manuscript with input from all authors.

References

- Herrmann JM & Köhl R (2007) Catch me if you can! Oxidative protein trapping in the intermembrane space of mitochondria. *J Cell Biol* **176**, 559–563.
- Pfanner N, Warscheid B & Wiedemann N (2019) Mitochondrial proteins: from biogenesis to functional networks. *Nat Rev Mol Cell Biol* **20**, 267–284.
- Tokatlidis K (2005) A disulfide relay system in mitochondria. *Cell* **121**, 965–967.
- Lu H, Allen S, Wardleworth L, Savory P & Tokatlidis K (2004) Functional TIM10 chaperone assembly is redox-regulated in vivo. *J Biol Chem* **279**, 18952–18958.
- Mesecke N, Terziyska N, Kozany C, Baumann F, Neupert W, Hell K & Herrmann JM (2005) A disulfide relay system in the intermembrane space of mitochondria that mediates protein import. *Cell* **121**, 1059–1069.
- Ceh-Pavia E, Spiller MP & Lu H (2013) Folding and biogenesis of mitochondrial small Tim proteins. *Int J Mol Sci* **14**, 16685–16705.
- Banci L, Bertini I, Calderone V, Cefaro C, Ciofi-Baffoni S, Gallo A, Kallergi E, Lionaki E, Pozidis C & Tokatlidis K (2011) Molecular recognition and substrate mimicry drive the electron-transfer process between MIA40 and ALR. *Proc Natl Acad Sci USA* **108**, 4811–4816.
- Hagiya M, Francavilla A, Polimeno L, Ihara I, Sakai H, Seki T, Shimonishi M, Porter KA & Starzl TE (1994) Cloning and sequence analysis of the rat augments of liver regeneration (ALR) gene: expression of biologically active recombinant ALR and demonstration of tissue distribution. *Proc Natl Acad Sci USA* **91**, 8142–8146.
- Farrell SR & Thorpe C (2005) Augments of liver regeneration: a flavin-dependent sulfhydryl oxidase with cytochrome *c* reductase activity. *Biochemistry* **44**, 1532–1541.
- Hell K (2008) The Erv1-Mia40 disulfide relay system in the intermembrane space of mitochondria. *Biochim Biophys Acta* **1783**, 601–609.
- Chatzi A & Tokatlidis K (2013) The mitochondrial intermembrane space: a hub for oxidative folding linked to protein biogenesis. *Antioxid Redox Signal* **19**, 54–62.
- Ang SK & Lu H (2009) Deciphering structural and functional roles of individual disulfide bonds of the mitochondrial sulfhydryl oxidase Erv1p. *J Biol Chem* **284**, 28754–28761.

- 13 Bien M, Longen S, Wagener N, Chwalla I, Herrmann JM & Riemer J (2010) Mitochondrial disulfide bond formation is driven by intersubunit electron transfer in Erv1 and proofread by glutathione. *Mol Cell* **37**, 516–528.
- 14 Tang X, Ang SK, Ceh-Pavia E, Heyes DJ & Lu H (2019) Kinetic characterisation of Erv1, a key component for protein import and folding in yeast mitochondria. *FEBS J* **287**, 1220–1231.
- 15 Levitan A, Danon A & Lisowsky T (2004) Unique features of plant mitochondrial sulfhydryl oxidase. *J Biol Chem* **279**, 20002–20008.
- 16 Eckers E, Petrungraro C, Gross D, Riemer J, Hell K & Deponte M (2013) Divergent molecular evolution of the mitochondrial sulfhydryl: cytochrome *c* oxidoreductase Erv in opisthokonts and parasitic protists. *J Biol Chem* **288**, 2676–2688.
- 17 Gross E, Sevier CS, Vala A, Kaiser CA & Fass D (2002) A new FAD-binding fold and intersubunit disulfide shuttle in the thiol oxidase Erv2p. *Nat Struct Mol Biol* **9**, 61–67.
- 18 Wang W, Winther JR & Thorpe C (2007) Erv2p: characterization of the redox behavior of a yeast sulfhydryl oxidase. *Biochemistry* **46**, 3246–3254.
- 19 Guo P-C, Ma J-D, Jiang Y-L, Wang S-J, Bao Z-Z, Yu X-J, Chen Y & Zhou C-Z (2012) Structure of yeast sulfhydryl oxidase Erv1 reveals electron transfer of the disulfide relay system in the mitochondrial intermembrane space. *J Biol Chem* **287**, 34961–34969.
- 20 Hofhaus G, Lee J-E, Tews I, Rosenberg B & Lisowsky T (2003) The N-terminal cysteine pair of yeast sulfhydryl oxidase Erv1p is essential for in vivo activity and interacts with the primary redox centre. *Eur J Biochem* **270**, 1528–1535.
- 21 Ceh-Pavia E, Ang SK, Spiller MP & Lu H (2014) The disease-associated mutation of the mitochondrial thiol oxidase Erv1 impairs cofactor binding during its catalytic reaction. *Biochem J* **464**, 449.
- 22 Ang SK, Zhang M, Lodi T & Lu H (2014) Mitochondrial thiol oxidase Erv1: both shuttle cysteine residues are required for its function with distinct roles. *Biochem J* **460**, 199–210.
- 23 Allen S, Balabanidou V, Sideris DP, Lisowsky T & Tokatlidis K (2005) Erv1 mediates the Mia40-dependent protein import pathway and provides a functional link to the respiratory chain by shuttling electrons to cytochrome *c*. *J Mol Biol* **353**, 937–944.
- 24 Dabir DV, Leverich EP, Kim SK, Tsai FD, Hirasawa M, Knaff DB & Koehler CM (2007) A role for cytochrome *c* and cytochrome *c* peroxidase in electron shuttling from Erv1. *EMBO J* **26**, 4801–4811.
- 25 Gerber J, Muhlenhoff U, Hofhaus G, Lill R & Lisowsky T (2001) Yeast ERV2p is the first microsomal FAD-linked sulfhydryl oxidase of the Erv1p/Alrp protein family. *J Biol Chem* **276**, 23486–23491.
- 26 Senkevich TG, White CL, Koonin EV & Moss B (2002) Complete pathway for protein disulfide bond formation encoded by poxviruses. *Proc Natl Acad Sci USA* **99**, 6667–6672.
- 27 Coppock DL, Kopman C, Scandalis S & Gilleran S (1993) Preferential gene expression in quiescent human lung fibroblasts. *Cell Growth Differ* **4**, 483–483.
- 28 Israel BA, Kodali VK & Thorpe C (2014) Going through the barrier: coupled disulfide exchange reactions promote efficient catalysis in quiescin sulfhydryl oxidase. *J Biol Chem* **289**, 5274–5284.
- 29 Schaefer-Ramadan S, Gannon SA & Thorpe C (2013) Human augmenter of liver regeneration: probing the catalytic mechanism of a flavin-dependent sulfhydryl oxidase. *Biochemistry* **52**, 8323–8332.
- 30 Quan S, Schneider I, Pan J, Von Hacht A & Bardwell JC (2007) The CXXC motif is more than a redox rheostat. *J Biol Chem* **282**, 28823–28833.
- 31 Wunderlich M & Glockshuber R (1993) Redox properties of protein disulfide isomerase (DsbA) from *Escherichia coli*. *Protein Sci* **2**, 717–726.
- 32 Krause G & Holmgren A (1991) Substitution of the conserved tryptophan 31 in *Escherichia coli* thioredoxin by site-directed mutagenesis and structure-function analysis. *J Biol Chem* **266**, 4056–4066.
- 33 Lu H & Woodburn J (2005) Zinc binding stabilizes mitochondrial Tim10 in a reduced and import-competent state kinetically. *J Mol Biol* **353**, 897–910.
- 34 Morgan B & Lu H (2008) Oxidative folding competes with mitochondrial import of the small Tim proteins. *Biochem J* **411**, 115–122.
- 35 Riemer J, Fischer M & Herrmann JM (2011) Oxidation-driven protein import into mitochondria: Insights and blind spots. *Biochim Biophys Acta* **1808**, 981–989.
- 36 Banci L, Bertini I, Ciofi-Baffoni S, Hadjiloi T, Martinelli M & Palumaa P (2008) Mitochondrial copper(I) transfer from Cox17 to Sco1 is coupled to electron transfer. *Proc Natl Acad Sci USA* **105**, 6803–6808.
- 37 Tienson HL, Dabir DV, Neal SE, Loo R, Hasson SA, Boontheung P, Kim SK, Loo JA & Koehler CM (2009) Reconstitution of the mia40-erv1 oxidative folding pathway for the small tim proteins. *Mol Biol Cell* **20**, 3481–3490.
- 38 Wang Q, Ang SK, Ceh-Pavia E, Pang J & Lu H (2015) Role of tryptophan residues of Erv1: Trp95 and Trp183 are important for its folding and oxidase function. *Biosci Rep* **35**, e00244.
- 39 Spiller MP, Ang SK, Ceh-Pavia E, Fisher K, Wang Q, Rigby SE & Lu H (2013) Identification and characterization of mitochondrial Mia40 as an iron-sulfur protein. *Biochem J* **455**, 27–35.